

NGC 3201 - Differential Extinction Map, Color-Magnitude Diagram, and Variable Star Candidates

Abstract

We present photometry results of our extensive monitoring project of the low-latitude Galactic globular cluster NGC 3201, one of approximately 15 globular clusters (GCs) we are probing for the existence of eclipsing binary systems. In order to obtain reliable photometry for the stars in the cluster, we created a differential reddening map to correct for the significant, variable extinction across the field-of-view. Our binary star detection analysis revealed 14 short-period variable stars in the field. 11 of these variable stars are eclipsing binaries, one is an RR Lyrae, and two are thus far unclassified systems. Among the eclipsing binaries stars, nine are of the W Ursa Majoris type, one an Algol system, and one a detached system. Using spectroscopic follow-up observations, we conclude that only one variable star (a W UMa type blue straggler) is a member of NGC 3201.

We present the extinction map described above, along with the dereddened, deep-photometry color-magnitude diagram (CMD) for NGC 3201, comprised of over 90 V and I images of the cluster. In addition, we show the phased lightcurves for all our variable star systems as well as their locations in the CMD and the field-of-view.

Introduction

The simultaneous analysis of photometry and spectroscopy data of eclipsing binary stars (EBs) in GCs may be used in the study of the dynamical evolution and formation of a cluster, e.g., by returning an estimate for the frequencies of binaries among main sequence stars and among blue stragglers. Moreover, this combination of photometry and spectroscopy data can serve as a tool to obtain direct distances to GCs and to calculate the Population II masses of the cluster member binary components. This distance determination method is free of intermediate calibration steps, can provide distances to tens of kpc, and may, in turn, be used to calibrate other distance determination methods (such as the L-[Fe/H] relation for RR Lyraes). If one assumes that a binary system has not suffered any mass loss from the system as a whole, then an unevolved (detached) system (no mass transfer between the components has taken place) will provide zero-age masses of the stars.

The main sources of uncertainty for the distance and mass determination are a) the relation between surface brightness and effective temperature of the stars, and b) the precise knowledge of interstellar extinction along the line-of-sight. NGC 3201 is located at low Galactic latitude (8.6 degrees), and we find that the differential extinction across the field-of-view varies by as much as 0.2 mag in E(V-I) (Figs 2 and 4).

We attempt to remove the differential extinction across NGC 3201 by finding average values for E(V-I) for CCD subregions of approximately 1 square arcmin in size with respect to a fiducial region in the field in which little or no differential reddening is taking place and where the overall extinction is low compared to the rest of the field. Using this technique and resulting reddening map (Fig 4), we obtain a high-quality, deep-photometry CMD of NGC 3201 (Fig 5).

Finally, we present the results of our search for photometrically varying binaries in NGC 3201 (Figs 1 & 6 through 9) in the form of the phased lightcurves of the variables as well as their locations in the field of view and the CMD of NGC 3201.

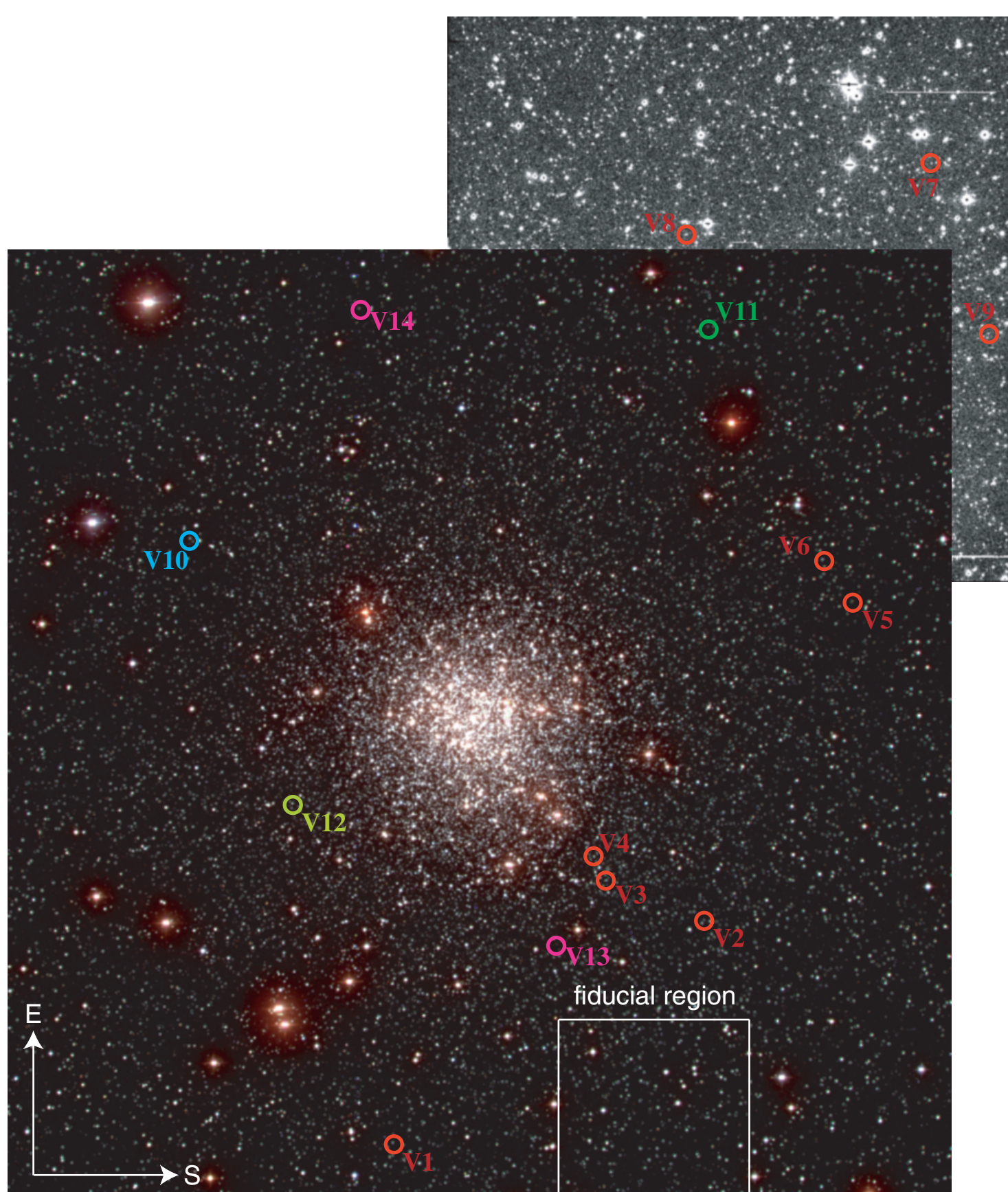


Fig. 1: Composite picture of two overlapping CCD fields of NGC 3201, taken at Las Campanas Observatory (LCO) 1m telescope (color picture, 23.5 arcmin on the side, centered on the cluster) and CTIO 0.9m telescope (BW picture, 13.5 arcmin on the side, centered on V11). The variable types (color coded) plus their locations are shown: W Ursa Majoris EB (V1-V9), RR Lyrae type (V10), Algol type EB (V11), detached EB (V12), unclassified systems (V13-V14). Note also the location of the fiducial region (in which little or no differential reddening is taking place) to which all the individual subregions were dereddened in the process of creating the differential extinction map (Fig. 4).

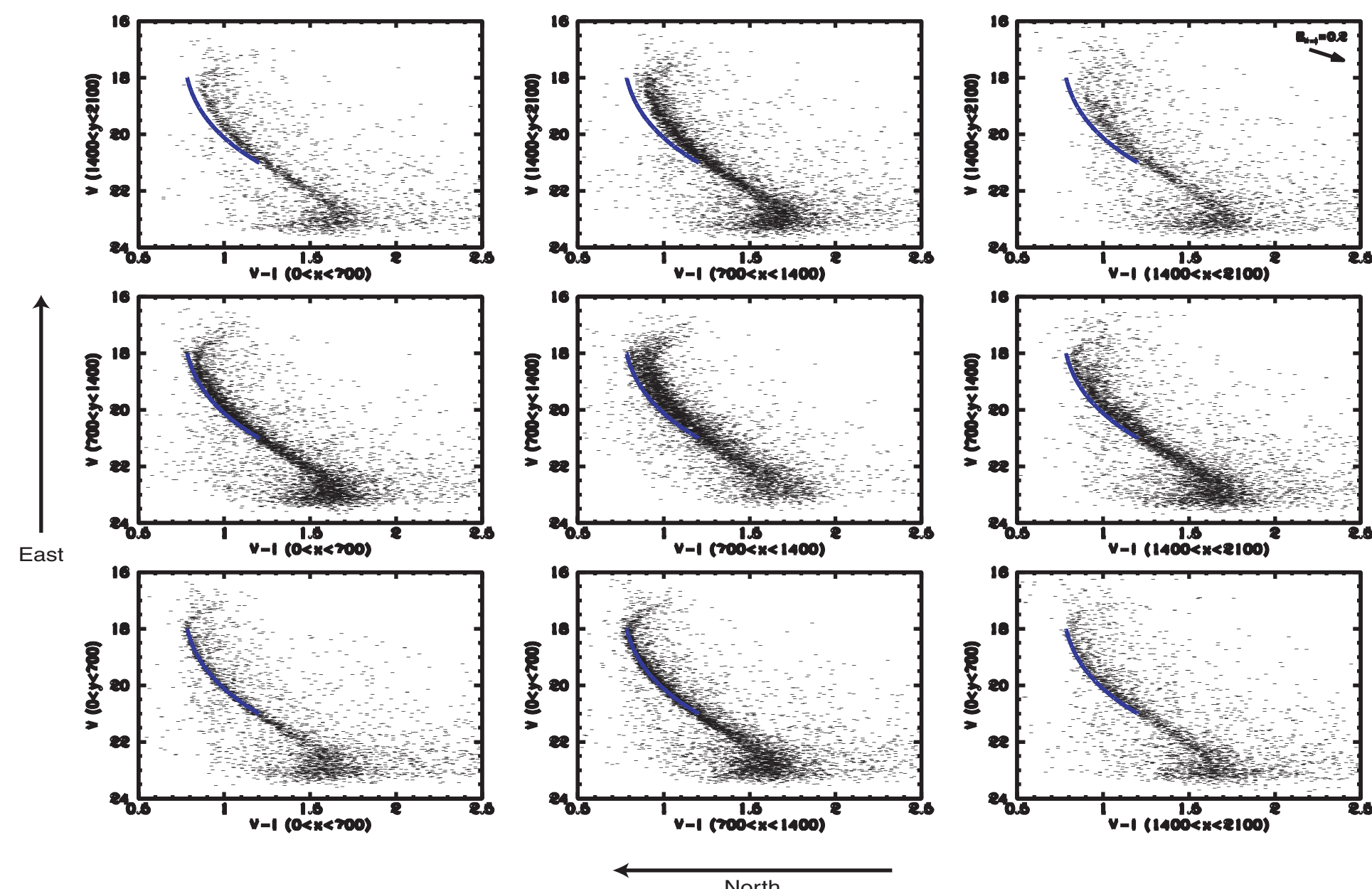


Fig. 2: Evidence of differential reddening across NGC 3201. For this image, the LCO field of view (see Fig. 1) was divided into nine subregions of the same size. The nine resulting CMDs are plotted in the respective panels in this figure (see axes labels for the coordinates of the individual subregion). The blue line in each of the nine panels represents the polynomial fit through the data points in the fiducial region $1200 < x < 1600$ and $0 < y < 400$ (see also Fig. 1). Note how not only the broadness of the main sequence changes with position, but also its location with respect to the fit, indicating the presence of differential extinction across the field-of-view. Note also that the fiducial region suffers little differential extinction (main sequence tight) and overall low extinction with respect to the rest of the field (main sequence falls to the red side of the fit in almost every panel).

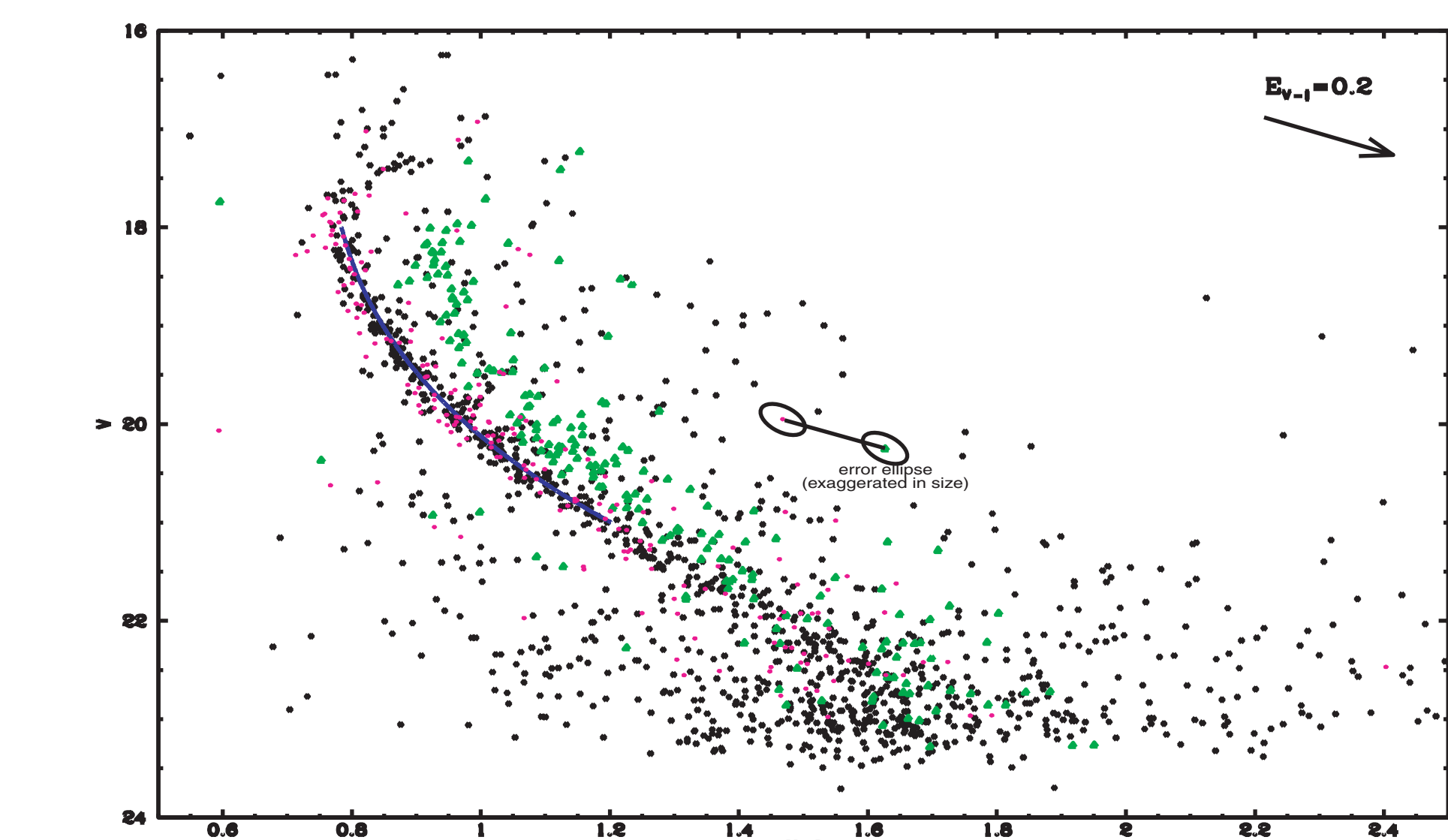


Fig. 3: Illustration of our dereddening procedure. The green datapoints represent the stars in a particular subregion of the CCD before being dereddened. The black symbols are the stars in the fiducial region where little/no differential extinction is taking place. The polynomial fit through the fiducial region stars is visible as the line with range $18 < V < 21$. Every star in the subregion is incrementally shifted along the reddening vector (shown in the top right corner of the figure) until it intersects the fit. The average shift of all the datapoints is then applied to the whole subregion. The purple symbols are the stars in the aforementioned subregion after being dereddened. One example case is shown in the middle of the figure along with associated error ellipses. The average differential E(V-I) for this subregion is approximately 0.2 mag. This procedure was repeated for every subregion of the CCD, enabling us to create the extinction map shown in Fig. 4.

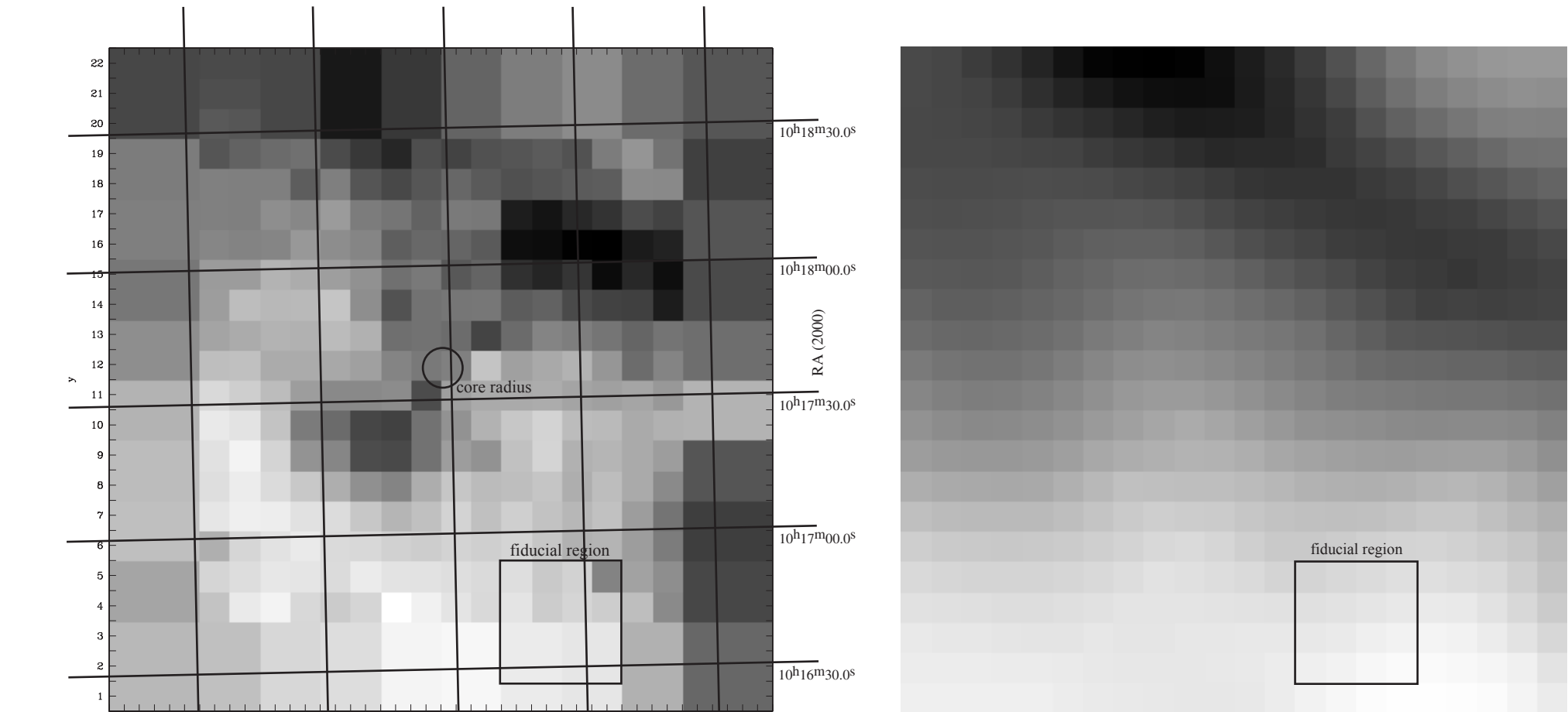


Fig. 4: Differential extinction map and SFD dust IR emissivity map. The left panel in this figure shows our extinction map with an overlaid coordinate system as well as the locations of the fiducial region and NGC 3201's core radius. Darker regions represent higher extinction relative to the average E(V-I) in the fiducial region. The size of every pixel in this map is approx. 1.2 square arcmin. The average E(V-I) relative to the fiducial region is ~86 mmag; the range in E(V-I) shown is approx. 0.2 mag. The right panel is a graphical representation of IR dust emissivity maps by Schlegel, Finkbeiner, and Davis (SFD), 1998. The orientation and size of the two maps are identical; we plotted the fiducial region onto the SFD map for reference. On a larger scale, the two maps look very similar. There are, however, smaller features which show up in our extinction map, but not in the SFD maps. Most likely, these are clumpy, cool regions of dust which were smoothed out in the SFD maps. The application of our extinction map to the CMD of NGC 3201 is illustrated in Fig. 5.

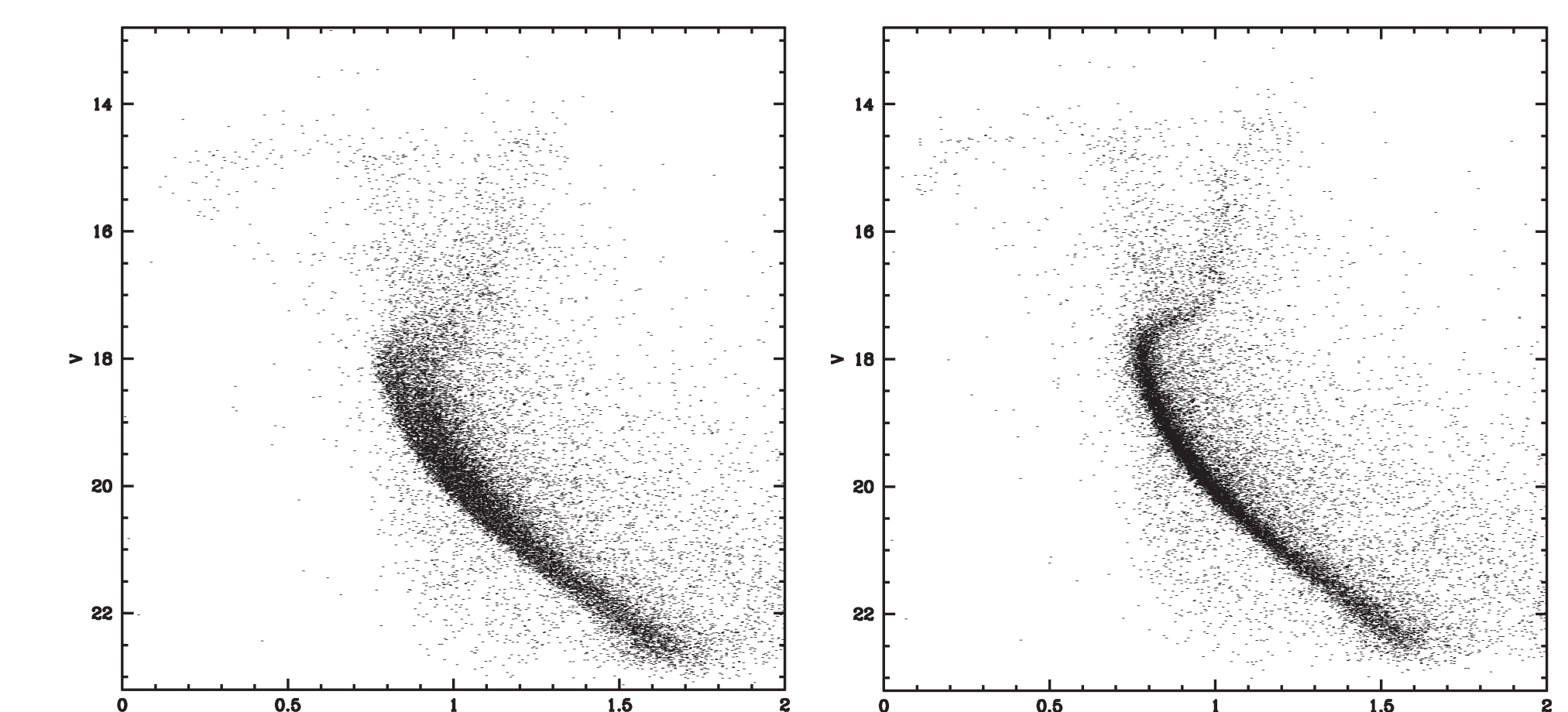


Fig. 5: Raw and differentially dereddened CMD of NGC 3201. The left panel in this figure shows the CMD of NGC 3201 before our extinction map was applied, the right one shows the differentially dereddened CMD. The datapoints are now shifted to the CMD location of the stars in the fiducial region, that is, no reddening zero point is applied. The improvement of the CMD appearance is immediately obvious: the width of the main sequence is reduced to a fraction of its "raw" value. The subgiant branch, hardly visible in the raw CMD, is well traced out by the datapoints. Even the horizontal branch, sparsely populated due to saturation effects, is narrower in the right panel.

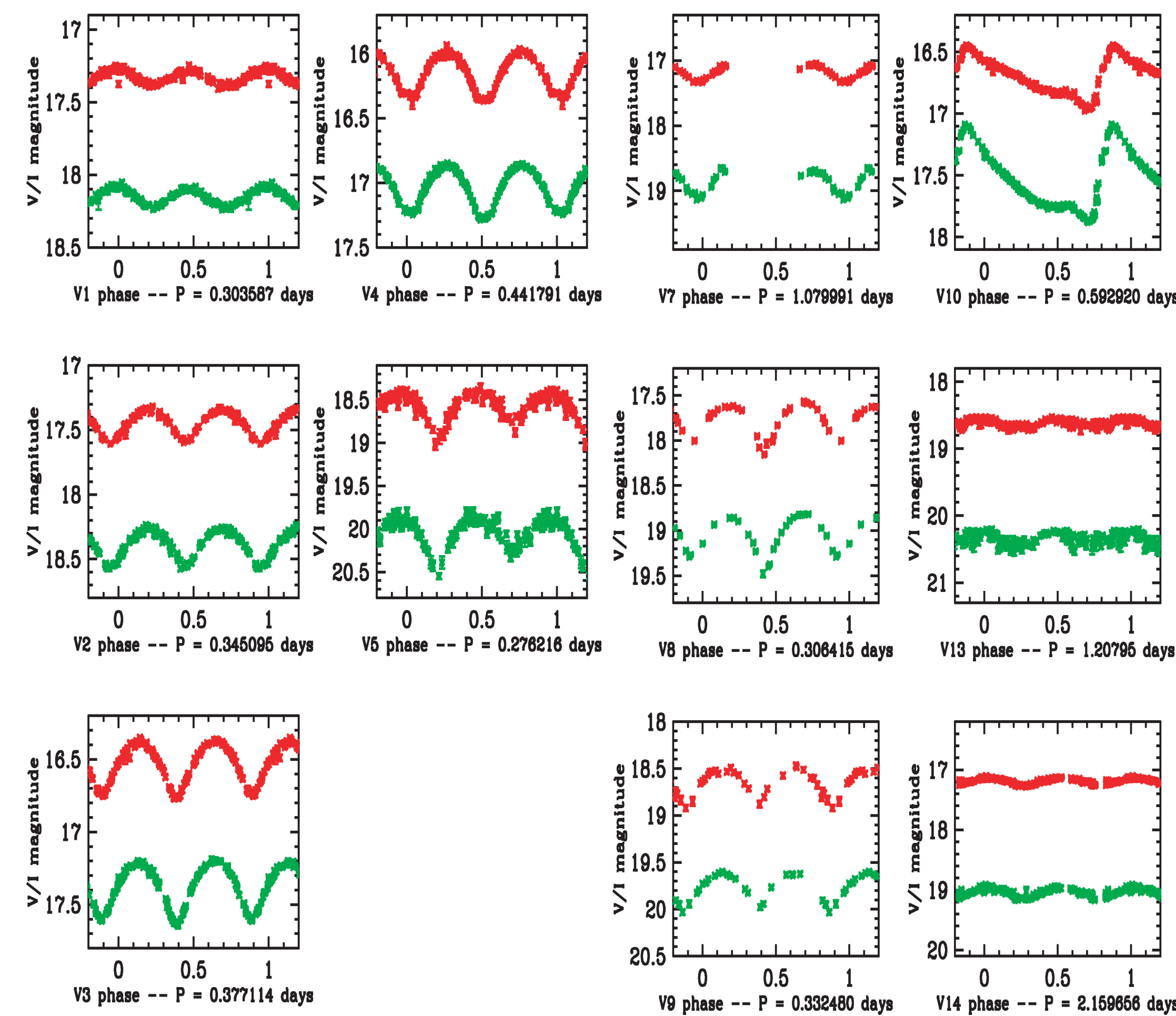


Fig. 6: Lightcurves of variable stars. The panels in this figure show the lightcurves of our W UMa binaries V1-5 and V7-9 (located in the CTIO field-of-view, see Fig. 1; note the sparser sampling of the lightcurves), the RR Lyrae (V10), and the two unclassified systems (V13-14). The 1 band data are plotted on top in each panel. Spectroscopy follow-up observations (see Additional Remarks) and the CMD of NGC 3201 (see Fig. 9) reveal that none of these variables is physically associated with the cluster.

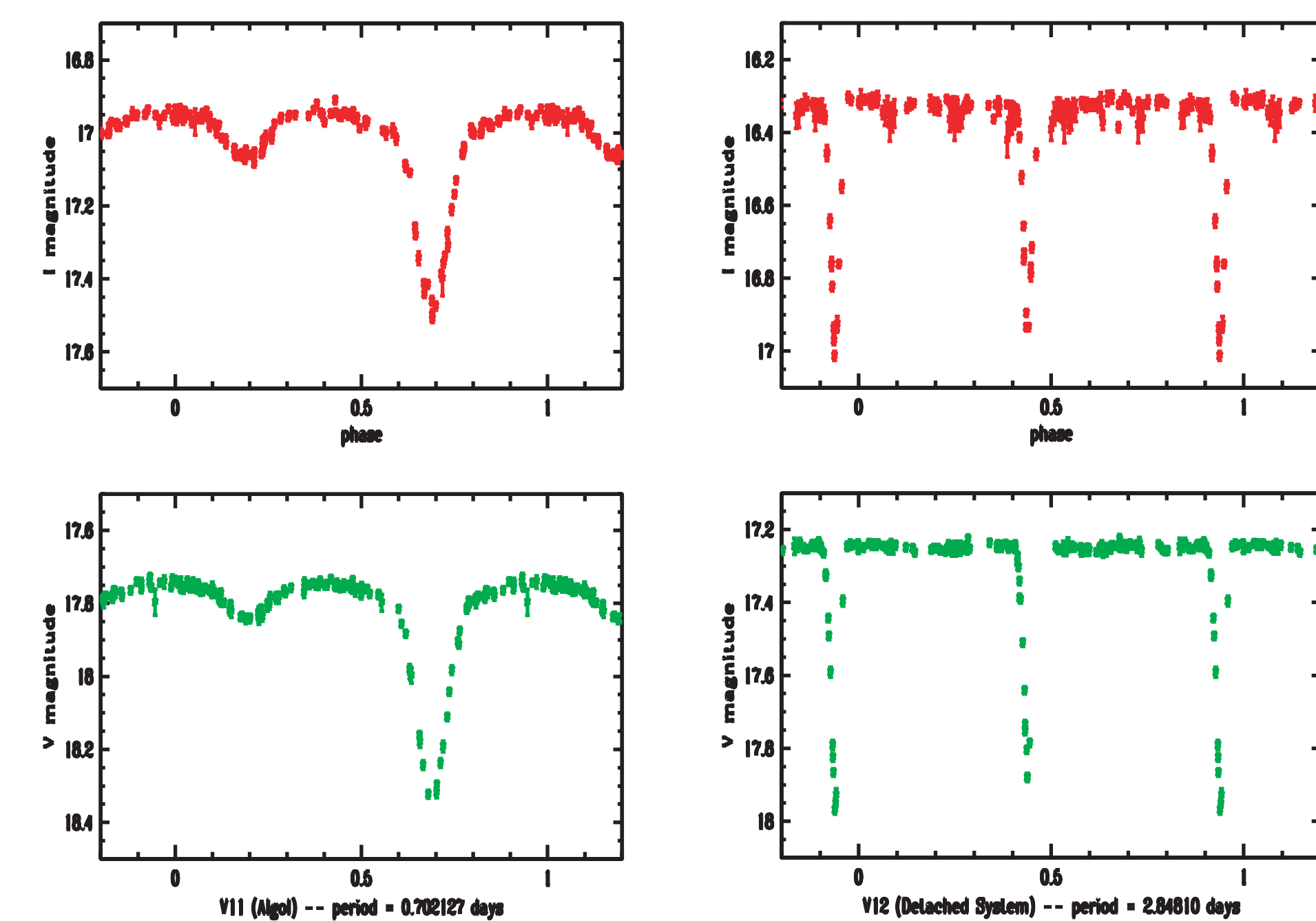


Fig. 7: Additional lightcurves of variable stars. The left panels in this figure show the V and I lightcurves of V11, the Algol type binary. The right panels display the lightcurves of V12, the detached binary system (recognizable by the presence of constant maximum light). Unfortunately, neither of these two binary systems is a member of NGC 3201 (see Additional Remarks).

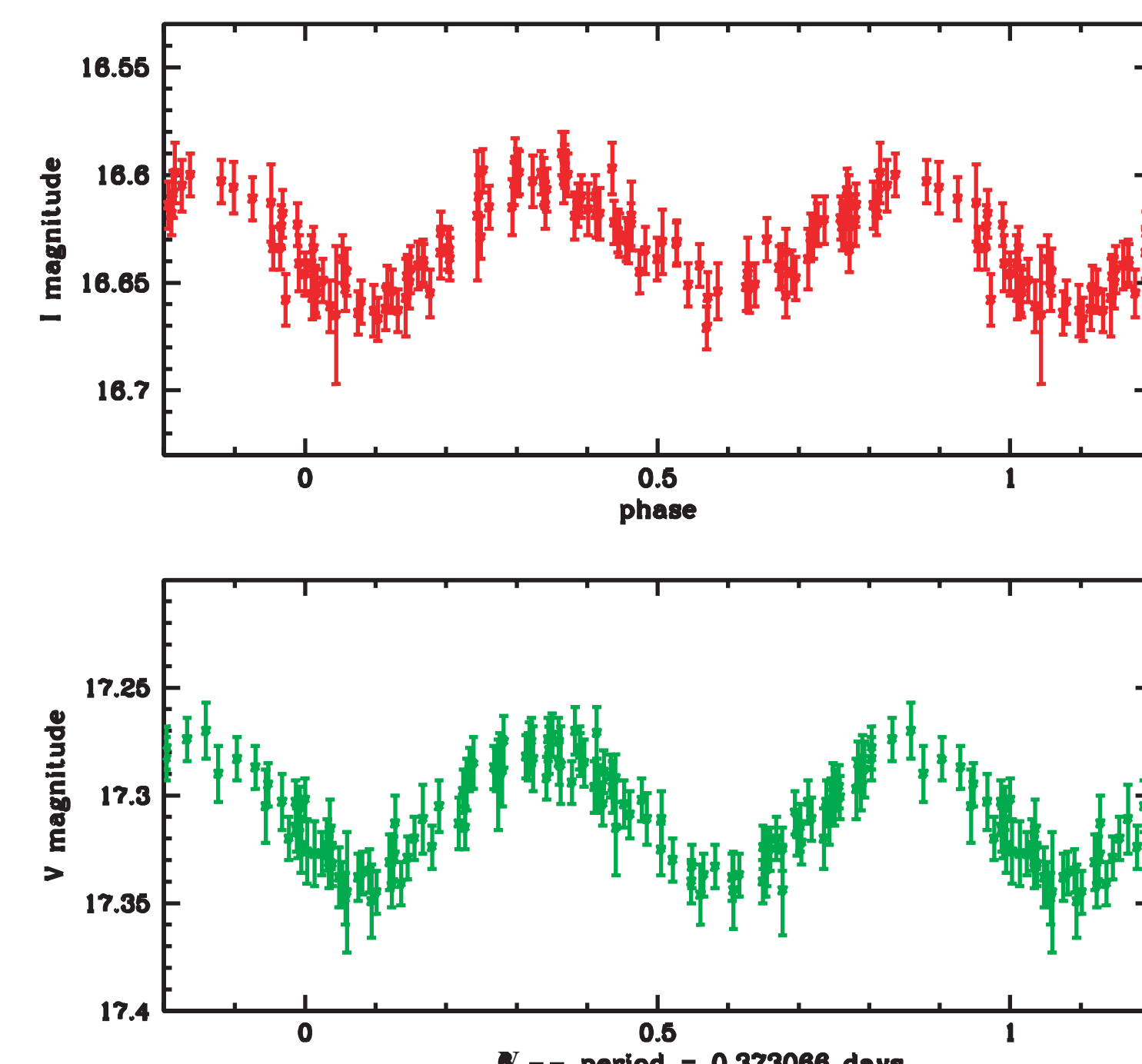


Fig. 8: Lightcurve of V6. The W UMa type binary V6, a blue straggler, proved to be the only variable star candidate in our sample which is a member of NGC 3201 (see Additional Remarks). Its V and I lightcurves are displayed here. Note the low amplitude, probably indicating a high angle of inclination of the system.

Kaspar von Braun
Mario Mateo
(University of Michigan)

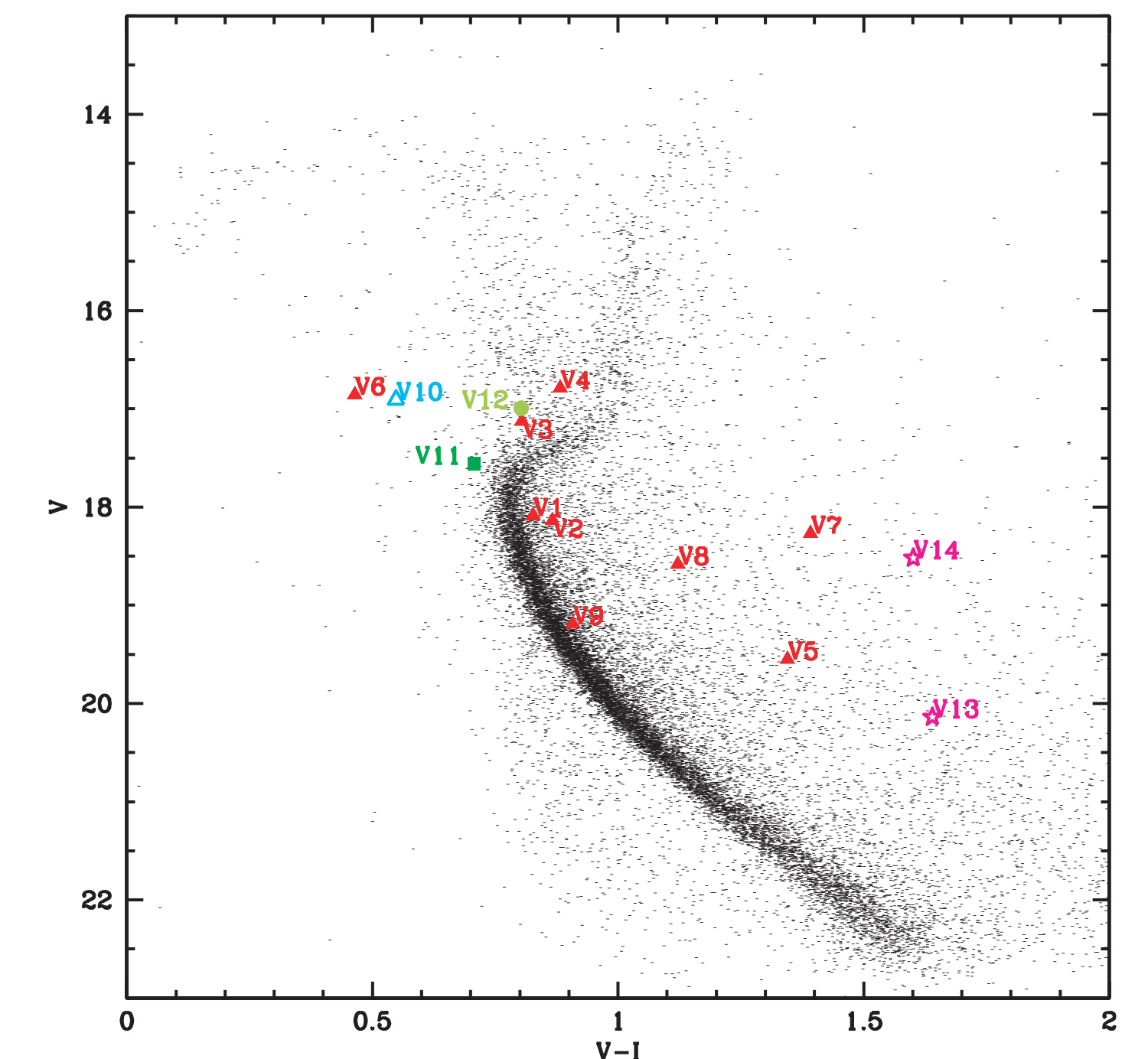


Fig. 9: NGC 3201's CMD with variables. The variable star candidates are plotted at maximum brightness in this figure. All data displayed are differentially dereddened (no reddening zero point applied). The colors indicate the variable type (see Fig. 1 and Table 1). The blue straggler V6 is the only variable which is a member of NGC 3201.

NGC 3201 Variable Star Candidates

Var. No	type	period (days)	RA (2000)	Dec (2000)	V(bright)	I(bright)
V1	W UMa	0.303587(28)	10:16:36.92	-46:22:29.3	18.054(17)	17.258(20)
V2	W UMa	0.345095(42)	10:17:07.73	-46:30:18.2	18.237(14)	17.319(19)
V3	W UMa	0.377114(43)	10:17:13.75	-46:27:54.7	17.189(21)	16.352(21)
V4	W UMa	0.44179(55)	10:17:17.18	-46:27:37.5	16.850(17)	15.965(22)
V5	W UMa	0.276216(31)	10:17:52.93	-46:34:06.7	19.847(21)	18.380(32)
V6	W UMa	0.37307(39)	10:17:59.08	-46:33:25.7	17.270(13)	16.599(19)
V7	W UMa	1.0800(90)	10:18:56.03	-46:36:10.4	18.658(15)	17.064(19)
V8	W UMa	0.30642(75)	10:18:31.97	-46:37:32.9	18.824(14)	17.577(19)
V9	W UMa	0.33248(61)	10:18:46.01	-46:30:13.8	19.609(22)	18.483(27)
V10	RR Lyrae	0.592920(53)	10:18:03.86	-46:17:48.7	17.088(12)	16.446(22)
V11	Algol	0.702127(99)	10:18:32.74	-46:30:42.5	17.728(13)	16.932(19)
V12	Detached	2.84810(98)	10:17:25.72	-46:20:12.4	17.225(14)	16.301(22)
V13	Unclass.	1.2080(44)	10:17:04.83	-46:26:39.7	20.203(35)	18.529(29)
V14	Unclass.	2.160(13)	10:18:36.28	-46:22:06.2	18.915(16)	17.108(21)

Table 1: Variable star candidates in the field of NGC 3201. The color indicates the type of variable star and is consistent with the colors used in Figs 1 and 9. Errors in parentheses indicate the uncertainty in the last two digits.

Additional Remarks

The GC NGC 3201 was probed for the existence of photometrically varying binary stars in the approximate magnitude range $16.5 < V < 20$, using around 300 epochs (600s exp time; approx. 45000 stars/image) in V and I, taken at the LCO 1m telescope between 1996 and 1998, roughly 70 epochs (600s exp time) taken at the CTIO 0.9m telescope in 2001 (Fig. 1), plus a number of shorter exposures to complete the CMD in the brighter regions. In order to precisely determine the magnitudes of the binaries, we created a differential reddening map for the cluster (Fig. 4), using a subset of our data (for a discussion on the calculation of the reddening zero point, see von Braun & Mateo, AJ, 121, 1522). We find that our extinction map agrees well with the dust emissivity maps by SFD, and detects additional, smaller scale dust features in the field. E(V-I) varies on a scale of arcminutes, with a range of 0.2 mag.

Our search for eclipsing binaries in NGC 3201 with periods between 0.2 and 5 days revealed the existence of 14 variable star candidates in the field (Figs 1, 6-9; Table 1). Our variability detection is based on a simple chi-squared algorithm with a few additional conditions (e.g., a correlated brightness variation in both bands). Periods for these candidates were determined using two independent methods: the minimum-string-length method as well as the analysis of variance. Both of these methods worked very well, especially in the case of smoothly varying variables, such as the RR Lyrae (V10) or the W UMa stars (V1-9). In the case of the Algol system (V11) and the detached system (V12), a final tweaking by hand (based on the appearance of the lightcurve) improved the precision of the period by seconds to a few tens of seconds.

While the question of cluster membership looks promising for a number of our variable stars, based on their location in the field-of-view and the CMD, a final verdict can only be given by spectroscopy. NGC 3201's distinct, retrograde systemic velocity is around 500 km/s. Follow-up spectroscopy obtained at the CTIO 4m telescope and Magellan 1 in 3/2001 showed that only one of the variables, V6 - a blue straggler W UMa binary, is a member of the GC.

Despite the fact that the large majority of the variable stars in our sample proved to be Galactic and not associated with NGC 3201, we have nevertheless shown the potential of our methods to successfully detect binaries, even with low amplitudes (V6) and duty cycles (V12), and to determine their periods to a precision of seconds. These tools, combined with our 1m telescope class photometry dataset and the capabilities of Magellan 1 for spectroscopy follow-up observations should enable us to detect binaries in the GCs in our sample (provided there are binaries in the clusters) and determine cluster membership for the southern and equatorial GC variables.